

D

Host Protein	Gene Name	Log ₂ Fold-Change	p-value
O00499	BIN1	8.390990101	0
O94966	USP19	6.51678174	0
Q04837	SSBP1	3.394890103	9.44E-09
Q8NBS9	TXNDC5	2.472638341	0.427798468
Q7RTV0	PHF5A	0.432961511	0.025103554

Figure S1

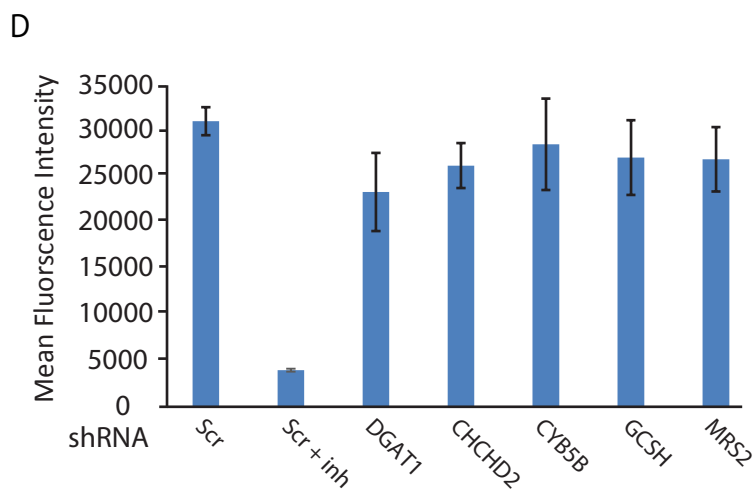
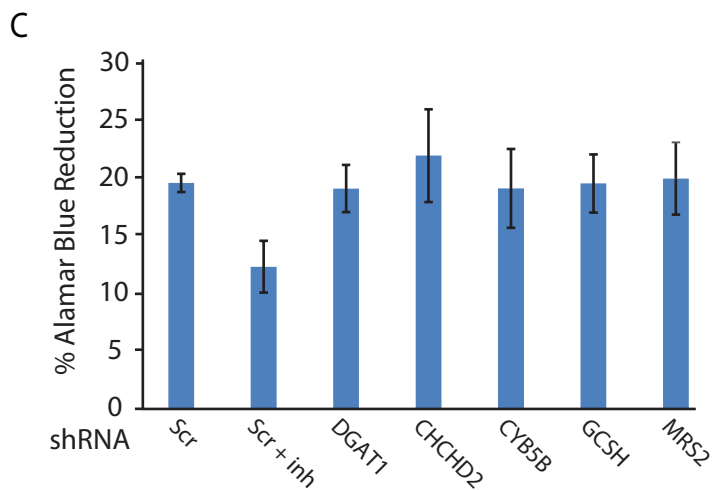
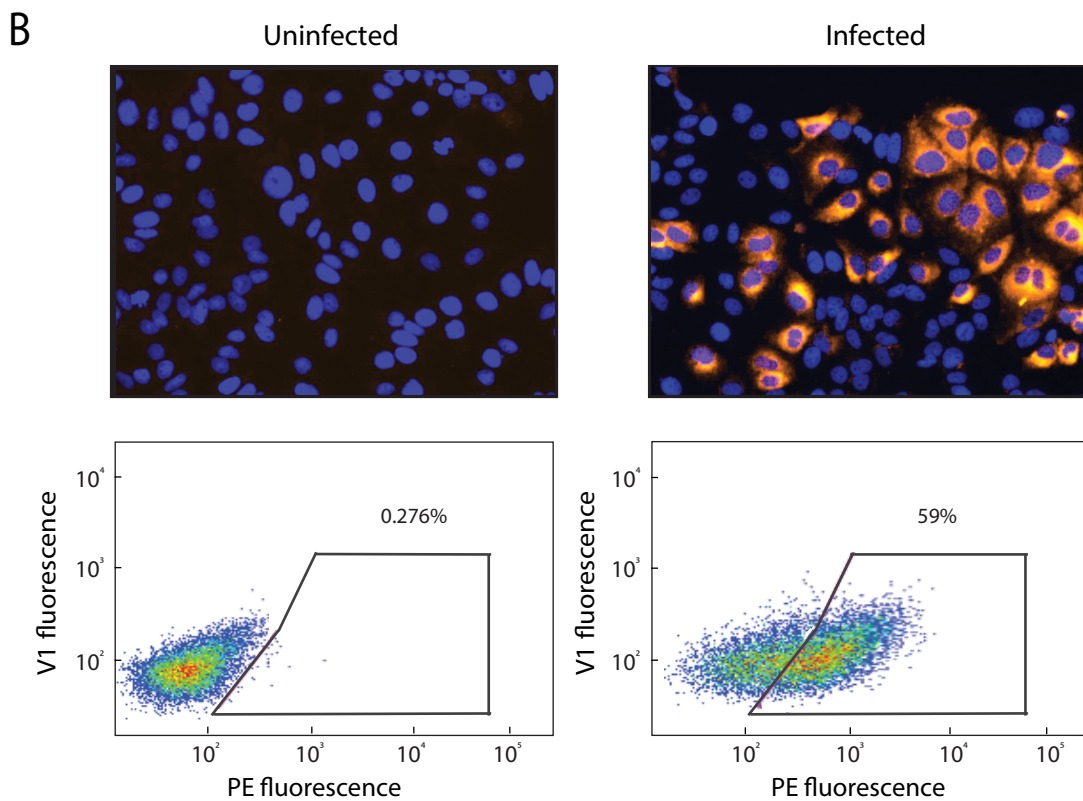
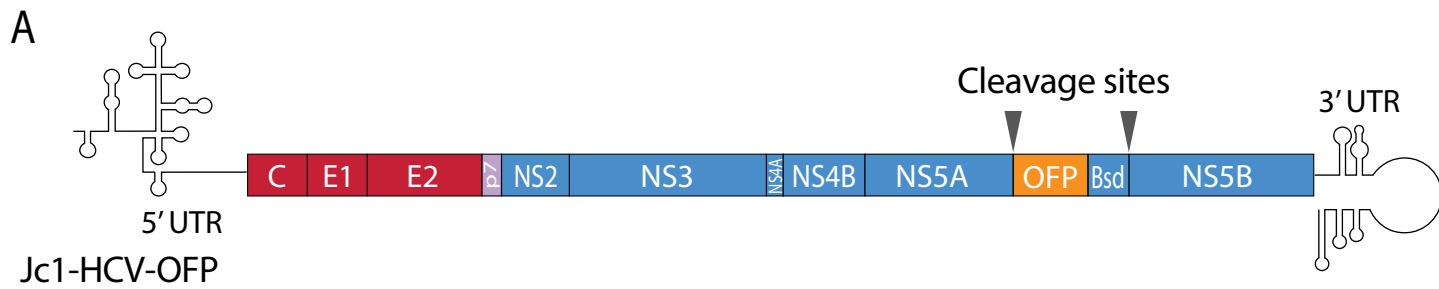


Figure S2

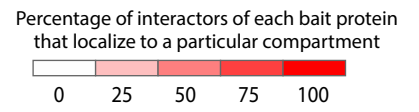
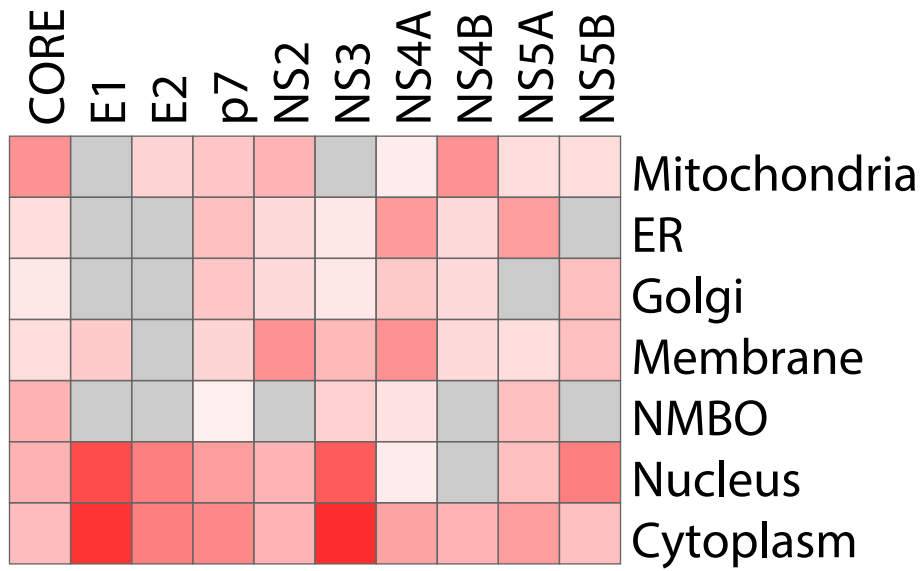
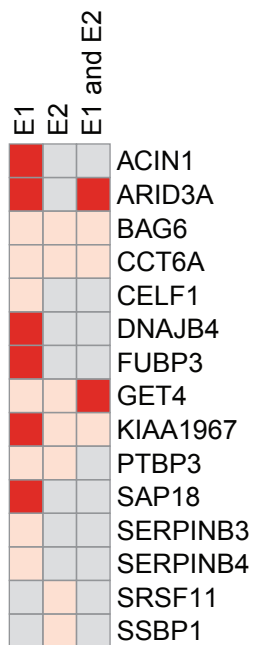
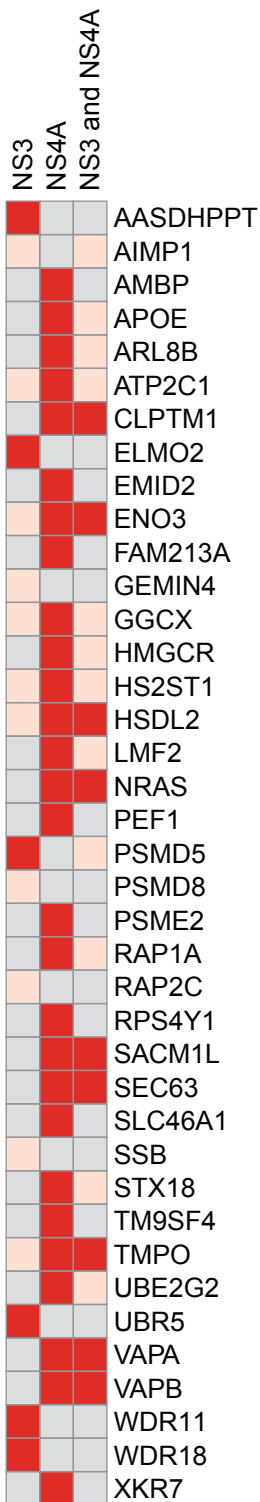


Figure S3

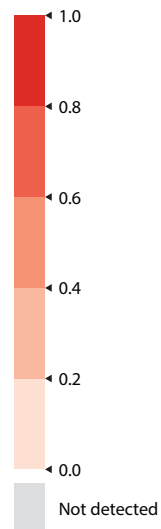
A



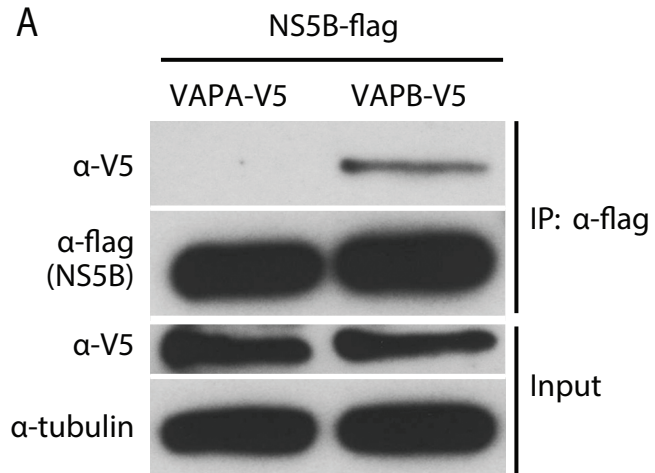
B



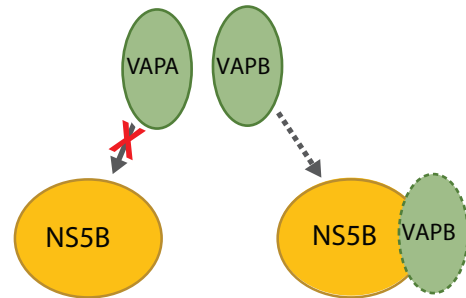
MiST Score



A

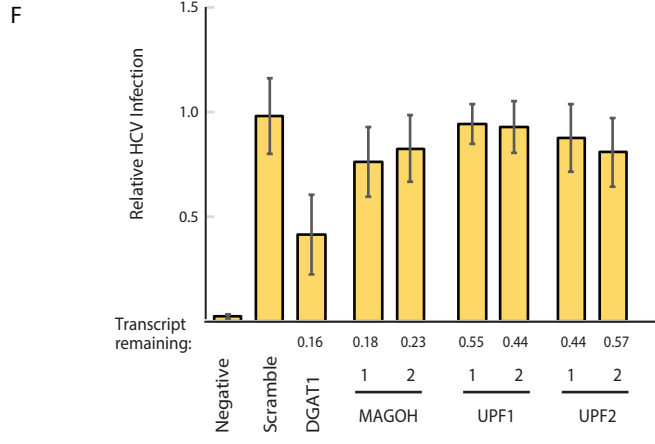
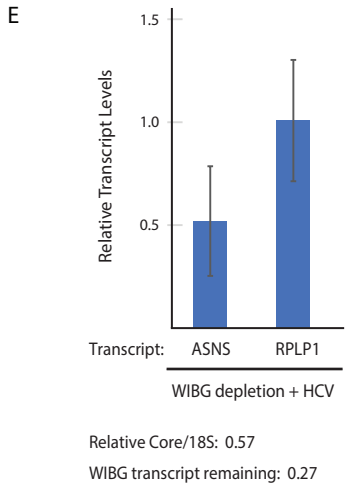
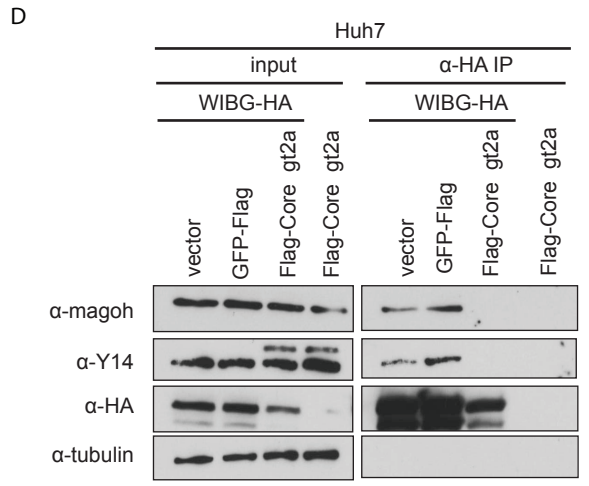
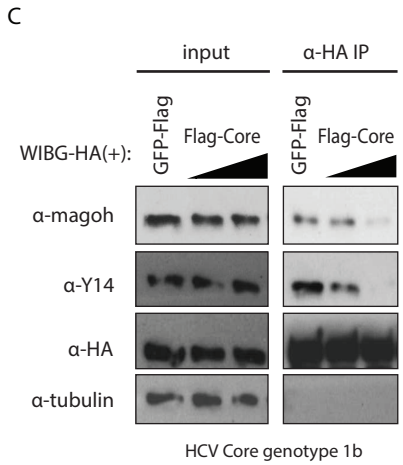
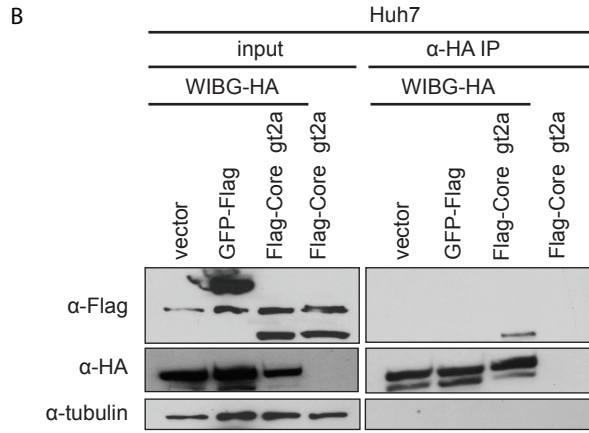
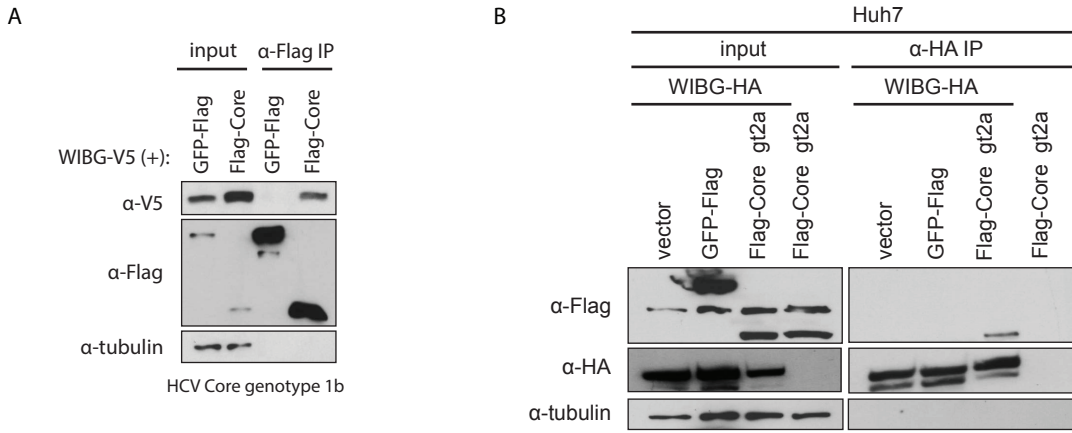


B



C

HCV Protein	Log ₂ Fold-Change	p-value
NS3	2.826	0
NS4A	6.302	0.000382
NS5A	-0.432	0.313976
NS5B	1.818	1.68E-13



HEK293T-HCV PPI Data

BAIT	PREY	MIST	COMPASS	Gene Name
NS4B	P61326	0.685510596	6.040105355	MAGOH, MAGOHA
NS4B	Q92900	0.194587717	3.890884815	UPF1, RENT1
Core	Q92900	0.240185763	4.159530831	UPF1, RENT1
E1	Q92900	0.260419766	3.762437201	UPF1, RENT1
E1	Q9BZ17	0.685510596	6.040105355	UPF3B, RENT3B
E2	Q92900	0.223165893	4.159530831	UPF1, RENT1
NS2	Q92900	0.159068828	2.941232457	UPF1, RENT1
p7	Q92900	0.581932085	6.452302517	UPF1, RENT1
Core	Q9Y5S9	0.78812827	20.03276316	Y14, RBM8A

Huh7-HCV PPI Data

BAIT	PREY	MIST	COMPASS	gene_name
E1	Q9Y5S9	0.429458	3.983252866	Y14, RBM8A
E1	Q92900	0.500968	4.225	UPF1, RENT1
E2	Q92900	0.336855	2.802547948	UPF1, RENT1
NS3	Q92900	0.43122	5.455760457	UPF1, RENT1
NS5A	Q92900	0.26951	3.787151723	UPF1, RENT1
NS5B	Q92900	0.239984	1.913548188	UPF1, RENT1
p7	Q92900	0.196973	1.913548188	UPF1, RENT1

Figure S6

Supplemental Figure Legends

Figure S1, related to Figures 1 and 3: Analysis of Interaction Data.

(A) A Venn diagram depicting the overlap of our refined interactome generated from Huh7 hepatoma cell data, our HEK293T data, and previously published AP/MS studies (Lamarre/Superti-Furga). (B) A Venn diagram depicting the overlap of our combined Huh7 and HEK293T data, previously published HCV-host PPI studies and RNAi studies. (C) An analysis of the overlap of host interactors identified with N or C-terminally tagged proteins. Due to protein expression concerns, there are cases in which only one (N or C-terminal) tag was used to generate interaction data. It is important to note that in most of these cases, the affinity tag is not located at the terminus that would be expected to disrupt membrane localization. For Core and NS5B, only N-terminally tagged HCV baits were used and for NS3, NS4A and p7 only C-terminally-tagged baits were used. (D) Mass spectrometry results of host proteins that co-immunoprecipitate with native NS5A in replicon-expressing Huh7.5 cells. Log₂ Fold-Change indicates the fold-enrichment of host proteins immunoprecipitated from HCV replicon-expressing cells as compared to the negative control, immunoprecipitations using the anti-NS5A antibody in Huh7.5 cells. The adjusted p-value is indicated and the data was obtained from three independent pull-downs

Figure S2, related to Figure 2: RNAi Infection Assay and Viability of Cells Depleted of Select Mitochondrial Factors.

Infection Assay with HCV Reporter Virus. (A) A schematic of the HCV-OFP (mKO2) (Jc1/^{NS5AB-OFP-Bsd}) reporter virus used in the shRNA infection screen. (B) The top panels show images (40X) of Huh7.5 cells with or without HCV-OFP infection. The bottom panels show the quantification by flow cytometry of HCV-infected or uninfected cells. The x-axis shows the PE (OFP) fluorescence

and the y-axis shows the V1 fluorescence, a negative control. (C, D) To analyze general cellular health, we used an alamar blue assay that results in the conversion of a dye to a fluorescent molecule when incubated with metabolically active cells. For assessment of mitochondrial viability we incubated cells with media containing CMXRos, a mitochondrial-specific fluorescent marker that is dependent on maintenance of the mitochondrial membrane potential. The percent reduction of alamar blue reagent, indicating the relative reducing capacity of the cells (C) or the mean fluorescence intensity of CMXRos, assessing mitochondrial membrane potential (D) is shown for cells in which the indicated transcripts are knocked down. Scramble shRNA is used as a negative control, while Scr + inh (CCCp, a disruptor of mitochondrial membrane potential) is used as a positive control for mitochondrial dysfunction. Shown are the average and standard deviation of three individual wells and the graphs are representative of two independent experiments.

Figure S3, related to Figure 4: Cellular Compartment Localization of Host Interactors. A heat map representing the percentage of interactors localized to the indicated cellular compartment for each bait protein. Cellular compartment localizations are not mutually exclusive, so each host protein may belong to multiple compartments.

Figure S4, related to Figure 5: Interactions of HCV E1 and E2, or NS3 and NS4A Expressed Individually or Together and Host Proteins Interacting with NS5A in HCV Replicon-Expressing Cells. (A) A heat map depicting the strength of interaction (MiST score) for all proteins interacting with E1 or E2 expressed individually on our refined map and the MiST score for those proteins with E1 and E2 expressed together. (B) A heat map depicting the strength of interaction (MiST score) for all proteins interacting with NS3 or NS4A expressed individually on our refined map and for those proteins with NS3 and NS4A expressed together.

Figure S5, related to Figure 5: NS5B Interacts with VAPB but not VAPA by Co-Immunoprecipitation and Interaction of VAPA with Native HCV Proteins in Replicon-

Expressing Cells. (A) Immunoprecipitations with α -flag resin of Huh7 cell lysates expressing flag-tagged HCV NS5B and either V5-tagged VAPA or VAPB demonstrates that NS5B interacts with VAPB, but not VAPA. (B) A model visualizing the immunoprecipitation results from (A). (C) Mass spectrometry results of HCV proteins that co-immunoprecipitate with native VAPA in replicon-expressing Huh7.5 cells. Log₂ Fold-Change indicates the fold-enrichment of host proteins immunoprecipitated from HCV replicon-expressing cells as compared to the negative control. The adjusted p-value is indicated and the data was obtained from three independent pull-downs.

Figure S6, related to Figure 6. Role of WIBG and NMD factors in HCV infection. (A) and (C) Immunoprecipitations in HEK293T cells expressing the indicated constructs along with the flag-tagged HCV core from genotype 1b. (B) and (D) Immunoprecipitations in Huh7 hepatoma cells expressing the indicated constructs along with the flag-tagged HCV core from genotype 2a. (E) Relative levels of NMD substrate (ASNS) and control (RPLP1) transcripts upon WIBG depletion during HCV infection. Two independent shRNAs were used to deplete WIBG (average transcript remaining is listed below) in Huh7.5 cells and cells were infected with HCV-OFP (SI) for six days. Results shown are averaged transcript levels (\pm SD) normalized to HCV-infected cells containing scramble shRNA. HCV infection rates in WIBG-depleted cells are indicated by relative core/18S ratio as compared to HCV-infected cells containing scramble shRNA. (F) Results of the HCV infection following knock-down of NMD factors and controls. NMD factors as well as the scramble (negative) and DGAT1 (positive) controls targeted with shRNAs are indicated on the x-axis. Relative infection levels (normalized to cell density) are indicated on the y-axis. Results are shown as average (\pm SD) of a minimum of six experiments (Experimental Procedures, S5). (G) Table summarizing interactions between several HCV proteins and NMD factors present in the HEK293T-HCV and Huh7-HCV PPI data along with MIST and COMPASS scores.

Supplemental Table Legends

Table S1, related to Figures 1 and 3. Summary of all AP/MS used to generate interaction data. The specific tagged HCV bait protein, cell type and mass spectrometry machine used for each sample is indicated. The summary provides the total number of immunoprecipitations analyzed for each cell type and machine type. LQT = Thermo Scientific LTQ XL linear ion trap mass spectrometer, VP = Thermo Scientific Velos Pro dual linear ion trap mass spectrometer

Table S2, related to Figures 1 and 3. Scores of all interactors identified in HEK293T cells. A summary of all COMPPASS scores and both iterations of MIST scores for all host proteins detected in HEK293T cells (worksheet 2). A description of columns is provided (worksheet 1).

Table S3, related to Figures 1 and 3. Scores of all interactors identified in Huh7 cells. A summary of all COMPPASS scores and both iterations of MIST scores for all host proteins detected in Huh7 cells (worksheet 2). A description of columns is provided (worksheet 1).

Table S4, related to Figure 2. RNAi screen candidates and RNAi screen results. The list of all interactors chosen for the RNAi screen, indicated by Uniprot and Gene Symbol (worksheet 1). The shRNA clones for each candidate are indicated by the TRC (The RNAi Consortium) number and were obtained from Sigma. Summary of the RNAi screen data generated for candidates with positive phenotypes (worksheet 2). Shown are results of the top two shRNA vectors for each host factor, including the average phenotype and standard deviation and the average transcript knock-down and standard deviation. Also indicated is the number of replicates performed for each shRNA construct.

Table S5, related to Figures 1 and S2. Summary of overlap statistics. Overlap of our study with previous RNAi and protein-protein interaction studies. Set description (worksheet 1) indicates published studies for which our dataset has overlap. Overlap general (worksheet 2) shows the numbers and p-values for the overlap between our study and previous HCV PPI or

RNAi studies. Overlap per method (worksheet 3) shows overlap between our PPI data and previous studies (AP/MS, yeast two hybrid (Y2H), and other literature). Overlap per method detail (worksheet 4) provides specific information about dataset overlaps for each method indicated.

Table S6, related to Figure 3. Interactor protein domain and function enrichment analysis.

We indicate the HCV bait protein, host prey proteins, average MIST score and average compass score associated with enriched function term (worksheet 1) or protein domain term (worksheet 2) in our Huh7 data. The number of preys for each term in our interactome and in our data set, as well as associated significance values are also indicated.

Supplemental Experimental Procedures

Plasmids Used in This Study

HCV ORFs were PCR-amplified from HCV JFH1 and cloned into the vector backbone pCDNA-TO (Invitrogen) carrying N- or C-terminal 3xFlag or 2xStrep-TagII sequences using SLIC cloning (Li and Elledge, 2012). Vectors expressing V5-tagged human proteins WIBG, VAPA, and VAPB were obtained from the Human Orfeome Collection (Yang et al., 2011). C-terminal HA-tagged WIBG was cloned into pCDNA3.1(+) using the NotI and XhoI restriction sites.

Plasmid source: Nevan J. Krogan

pcDNA4/TO N-term 2Xstrep - pcDNA4/TO (Invitrogen) carrying an N-terminal 2XstrepTagII sequence

pcDNA4/TO C-term 2Xstrep - pcDNA4/TO (Invitrogen) carrying an C-terminal 2XstrepTagII sequence

pcDNA4/TO N-term 3Xflag - pcDNA4/TO (Invitrogen) carrying an N-terminal 3Xflag sequence

pcDNA4/TO C-term 3Xflag - pcDNA4/TO (Invitrogen) carrying an C-terminal 3Xflag sequence

Plasmid source: This study

pHR301 - HCV 2A p7 C-terminal 2X strep

pHR302 - HCV 2A NS2 C-terminal 2X strep

pHR304 - HCV 2A E1 C-terminal 2X strep
pHR308 - HCV 2A NS2 N-terminal 2X strep
pHR309 - HCV 2A NS3 C-terminal 2X strep
pHR310 - HCV 2A NS4A C-terminal 2X strep
pHR311 - HCV 2A NS4A N-terminal 2X strep
pHR312 - HCV 2A NS5A C-terminal 2X strep
pHR313 - HCV 2A NS4B N-terminal 3X flag
pHR314 - HCV 2A p7 N-terminal 3X flag
pHR315 - HCV 2A NS2 N-terminal 3X flag
pHR316 - HCV 2A E1 N-terminal 3X flag
pHR317 - HCV 2A NS4A N-terminal 3X flag
pHR318 - HCV 2A E2 N-terminal 3X flag
pHR319 - HCV 2A Core N-terminal 3X flag
pHR320 - HCV 2A NS5A N-terminal 3X flag
pHR321 - HCV 2A NS2 C-terminal 3X flag
pHR322 - HCV 2A NS4A C-terminal 3X flag
pHR323 - HCV 2A NS4B C-terminal 3X flag
pHR324 - HCV 2A E1 C-terminal 3X flag
pHR325 - HCV 2A p7 C-terminal 3X flag
pHR326 - HCV 2A NS4B C-terminal 2X strep
pHR327 - HCV 2A NS4B N-terminal 2X strep
pHR328 - HCV 2A NS5A N-terminal 2X strep
pHR329 - HCV 2A E2 C-terminal 3X flag
pHR330 - HCV 2A NS5A C-terminal 3X flag
pHR331 - HCV 2A NS3 C-terminal 3X flag
pHR350 - HCV 2A NS5B (codon optimized by GenScript) N-terminal 3X flag
WIBG-HA – pCDNA3.1(+) Hs_WIBG C-terminal 1X HA tag

Plasmid source: CCSB Human ORFeome Collection v8.1 (Thermo Scientific)

VAPA-V5 - Hs_VAPA in pLX304 (ccsbBroad304_11349)

VAPB-V5 - Hs_VAPB in pLX304 (ccsbBroad304_11349)

WIBG-V5 - Hs_WIBG in pLX304 (ccsbBroad304_023)

Primers for Cloning Vectors Used in This Study		
Construct	Forward Primer	Reverse Primer
HCV 2A p7 C-terminal 2X strep	CAGTGTGGTGGAAATTCGCCGCCATGGCATTGGAGAAGTTGGTCTGT	CTCCCTCGAGCGGCCCGCACGGCATAAGCCTGCCGGGGC
HCV 2A NS2 C-terminal 2X strep	CAGTGTGGTGGAAATTCGCCGCCATGTATGACGCACCTGTGCACGG	CTCCCTCGAGCGGCCCGCACAAAGGAGCTTCACCCCTTGG
HCV 2A E1 C-terminal 2X strep	CTCCCTCGAGCGGCCCGCACCGCGTCCACCACAGCGGCCA	CAGTGTGGTGGAAATTCGCCGCCATGGCCCAGGTGAAGAATACCAG
HCV 2A NS2 N-terminal 2X strep	CCAGTTCGAGAAGGGGGCGGCCGCTTATGACGCACCTGTGCACGG	GGTTTAAACGGGCCCTCTAGATAAGGAGCTTCCACCCCTTGG
HCV 2A NS3 C-terminal 2X strep	CAGTGTGGTGGAAATTCGCCGCCATGGCTCCCATCACTGCTTATGC	CTCCCTCGAGCGGCCCGCACGGTCATGACCTCAAGGTCAG
HCV 2A NS4A C-terminal 2X strep	CAGTGTGGTGGAAATTCGCCGCCATGAGCACGTGGGTCCTAGCTGG	CTCCCTCGAGCGGCCCGCACGCATTCCCTCCATCTCATCAA
HCV 2A NS4A N-terminal 2X strep	CCAGTTCGAGAAGGGGGCGGCCGCTAGCACGTGGGTCCTAGCTGG	GGTTTAAACGGGCCCTCTAGATGCATTCCCTCATCTCATCAA
HCV 2A NS5A C-terminal 2X strep	CAGTGTGGTGGAAATTCGCCGCCATGTCCGGATCCTGGCTCCGCGA	CTCCCTCGAGCGGCCCGCACGCAGCACACGGTGGTATCGT
HCV 2A NS4B N-terminal 3X flag	CCAGTTCGAGAAGGGGGCGGCCGCTGCCTCTAGGGCGGCTCTCAT	GGTTTAAACGGGCCCTCTAGATGCATGGGATGGGGCAGTCCT
HCV 2A p7 N-terminal 3X flag	CCAGTTCGAGAAGGGGGCGGCCGCTGCATGGAGAAGTTGGTCTGT	GGTTTAAACGGGCCCTCTAGATGGCATAAGCCTGCCGGGGCA
HCV 2A NS2 N-terminal 3X flag	CCAGTTCGAGAAGGGGGCGGCCGCTTATGACGCACCTGTGCACGG	GGTTTAAACGGGCCCTCTAGATAAGGAGCTTCCACCCCTTGG
HCV 2A E1 N-terminal 3X flag	CCAGTTCGAGAAGGGGGCGGCCGCTGCCAGGTGAAGAATACCAG	GGTTTAAACGGGCCCTCTAGATCGCGTCCACCCAGCGGCCA
HCV 2A NS4A N-terminal 3X flag	CCAGTTCGAGAAGGGGGCGGCCGCTAGCACGTGGGTCCTAGCTGG	GGTTTAAACGGGCCCTCTAGATGCATTCCCTCATCTCATCAA
HCV 2A E2 N-terminal 3X flag	CCAGTTCGAGAAGGGGGCGGCCGCTGGCACACCACCGTTGGAGG	GGTTTAAACGGGCCCTCTAGATTGCTTCGGCCTGGCCCAACA
HCV 2A Core N-terminal 3X flag	CCAGTTCGAGAAGGGGGCGGCCGCTAGCAAAATCCTAAACCTCA	GGTTTAAACGGGCCCTCTAGATAGCAGAGACCGGAACGGTGA
HCV 2A NS5A N-terminal 3X flag	CCAGTTCGAGAAGGGGGCGGCCGCTCCGGATCCTGGCTCCGCGA	GGTTTAAACGGGCCCTCTAGATGCAGCACACGGTGGTATCGT
HCV 2A NS2 C-terminal 3X flag	CAGTGTGGTGGAAATTCGCCGCCATGTATGACGCACCTGTGCACGG	CTCCCTCGAGCGGCCCGCACAAAGGAGCTTCACCCCTTGG
HCV 2A NS4A C-terminal 3X flag	CAGTGTGGTGGAAATTCGCCGCCATGAGCACGTGGGTCCTAGCTGG	CTCCCTCGAGCGGCCCGCACGCATTCCCTCCATCTCATCAA

HCV 2A NS4B C-terminal 3X flag	CAGTGTGGTGGAAATTCGCCGCCATGGCCTC TAGGGCGGCTCTCAT	CTCCCTCGAGCGGCCCGCACGCATGGGAT GGGGCAGTCCT
HCV 2A E1 C-terminal 3X flag	CTCCCTCGAGCGGCCCGCACCGCGTCCACC CCAGCGGCCA	CAGTGTGGTGGAAATTCGCCGCCATGGCCC AGGTGAAGAATACCAG
HCV 2A p7 C-terminal 3X flag	CAGTGTGGTGGAAATTCGCCGCCATGGCATT GGAGAAGTTGGTCGT	CTCCCTCGAGCGGCCCGCACGGCATAAGCC TGCCGGGGC
HCV 2A NS4B C-terminal 2X strep	CAGTGTGGTGGAAATTCGCCGCCATGGCCTC TAGGGCGGCTCTCAT	CTCCCTCGAGCGGCCCGCACGCATGGGAT GGGGCAGTCCT
HCV 2A NS4B N-terminal 2X strep	CCAGTTCGAGAAGGGGGCGGCCGCTGCCT CTAGGGCGGCTCTCAT	GGTTTAAACGGGCCCTCTAGATGCATGGG ATGGGGCAGTCCT
HCV 2A NS5A N-terminal 2X strep	CCAGTTCGAGAAGGGGGCGGCCGCTTCCG GATCCTGGCTCCGCGA	GGTTTAAACGGGCCCTCTAGATGCAGCAC ACGGTGGTATCGT
HCV 2A E2 C-terminal 3X flag	CTCCCTCGAGCGGCCCGCACTGCTTCGGCC TGGCCCAACA	CAGTGTGGTGGAAATTCGCCGCCATGGGCA CCACCACCGTTGGAGG
HCV 2A NS5A C-terminal 3X flag	CAGTGTGGTGGAAATTCGCCGCCATGTCCGG ATCCTGGCTCCGCGA	CTCCCTCGAGCGGCCCGCACGCAGCACAC GGTGGTATCGT
HCV 2A NS3 C-terminal 3X flag	CAGTGTGGTGGAAATTCGCCGCCATGGCTCC CATCACTGCTTATGC	CTCCCTCGAGCGGCCCGCACGGTCATGACC TCAAGGTCAG
HCV 2A NS5B (codon optimized by GenScript) N-terminal 3X flag	TTGCGGCCGCTATGTCAATGTCATACTCCT G	TTTCTAGATTAGCGGGCAGGCAGCAGAA
Hs_WIBG-HA	CGGCGGCCGCATGGAAGCTGCCGGCAGCC	GCCTCGAGTCACGCATAGTCAGGTACATC GTATGGGTAAGCCATGAGGCCTAACTCCA AGTCCTCTAACTCC

Amino Acid Sequences of Proteins Used in This Study

core HCV Genotype 2A

STNPKPQRKTKRNTNRRPEDVKFPGGGQIVGGVYLLPRRGPRLGVRTTRKTSERSQPRGRRQ
PIPKDRRSTGKAWGKPGRPWPLYGNEGLWAGWLLSPRGSRPSWGPTDPRHRSRNVGKVI
DTLTCGFADLMGYIPVVGAPLSGAARAVAHGVRVLEDGVNYATGNLPGFPFSIFLLALLSCITVP
VSA

E1 HCV Genotype 2A

QVKNTSSSYMVTNDCSNDISITWQLEAAVLHVPGCVPCERVGNTSRCWVPVSPNMAVRQPGA
LTQGLRTHIDMVMSATFCSALYVGDLCGGVMLAAQVFIVSPQYHWFVQECNCSIYPGTITGH
RMAWDMMMNSPTATMILAYVMRVPEVIIDIVSGAHWGVFMFLAYFSMQGAWAKVIVILLAA
GVDA

E2 HCV Genotype 2A

GTTTVGGAVARSTNVIAGVFSHGPPQNIQLINTNGSWHINRTALNCNDSLNTGFLAALFYTNRF
NSSGCPGRLSACRNIEAFRIGWGTLQYEDNVTNPEDMRPYCWHYPPKPCGVVPARSVCGPV
YCFTPSPVVVGTTDRRGVPTYTWGENETDVLLNSTRPPQGSWFGCTWMNSTGFTKTCGAP

PCRTRADFNASTDLLCPTDCFRKHPDATYIKCGSGPWLTpkclvhypyrllwhypctvnftifki
RMYVGGVEHRLTAACNFRGDRCDLEDRDRSQLSPLLHSTTEWAILPCTYSDLPALSTGLLHL
HQNIVDVQYMYGLSPAITYVVRWEWVLLFLLADARVCACLWMLILLGQAEA

p7 HCV Genotype 2A

ALEKLVVLAHAASAANCHGLLYFAIFFVAAWHIRGRVVPLTTYCLTGLWPFCLLLMALPRQAYA

NS2 HCV Genotype 2A

YDAPVHGQIGVGLLILITLFTLTPGYKTLLGQCLWWLCYLLTLGEAMIQEWVPPMQVRGGRDGI
AWAVTIFCPGVVFDITKWLLALLGPAYLLRAALTHVPYFVRAHALIRVCALVKQLAGGRYVQVAL
LALGRWTGTYYDHLTPMSDWAASGLRDLAVAVEPIIFSPMEKKVIVWGAETAACGDILHGLPV
SARLGQEILLGPADGYTSKGWKL

NS3 HCV Genotype 2A

APITAYAQQTRGLLGAIVVSMTGRDRTEQAGEVQILSTVSQSFLGTTISGVLWTVYHGAGNKT
AGLRGPVTQMYSSAEGDLVGWPSPPGKTSLEPCKCGAVDLYLVTRNADVIPARRRGDKRGAL
LSPRPISLTKGSSGGPVLCPRGHVVGFRFAAVCSRGVAKSIDFIPVETLDVVTRSPFTSDNSTPP
AVPQTYQVGYLHAPTGSKSTKVPVAYAAQGYKVLVLPNSVAATLGFGAYLSKAHGINPNIRT
GVRTVMTGEAITYSTYGKFLADGGCASGAYDIIICDECHAVDATSILGIGTVLDQAETAGVRLTVL
ATATPPGSVTTTPHDIEEVGLGREGEIPFYGRAIPLSCIKGGRHLIFCHSKKKCEDELAALRGMG
LNAVAYYRGLDVSIIPAQGDVVVATDALMTGYTGDFDSVIDCNVAVTQAVDFSLDPTFTITTQT
VPQDAVSRSRQRRTGRGRQGTYYRYVSTGERASGMFDSVVLCECYDAGAAWYDLTPAETTV
RLRAYFNTPLPVCQDHLFEWAVFTGLTHIDAHFLSQTKQAGENFAYLVAYQATVCARAKAP
PPSWDAMWKCLARLKPTLAGPTPLLYRLGPITNEVTLTHPGTKYIATCMQADLEVMT

NS4A HCV Genotype 2A

STWVLAGGVLAAVAAYCLATGCVSIIGRLHVNQRVVVAPDKEVLYEAFDEMEEC

NS4B HCV Genotype 2A

ASRAALIEEGQRIAEMLKSKIQGLLQQASKQAQDIQPAMQASWPKVEQFWARHMWNFISGIQY
LAGLSTLPGNPAVASMMAFSAALTSPLSTSTTILLNIMGGWLASQIAPPAGATGFVVSGLVGAA
VGSIGLGKVLVDILAGYGAGISGALVAFKIMSGEKPSMEDVINLLPGILSPGALVVGVICAILRRH
VGPGEAVQWMNRLIAFASRGNHVAPTHYVTESDASQRVTQLLGSLLTITSLRRLHNWITEDC
PIPC

NS5A HCV Genotype 2A

SGSWLRDWDVWCTILTDFKNWLTSKLFKLPGLPFISCQKGYKGVWAGTGIMTTRCPCGANI
SGNVRLGSMRITGPKTCMNTWQGTFFPINCYTEGQCAPKPPTNYKTAIWRVAASEYAEVTQH
SYSYVTGLTTDNLKIPCQLPSPEFFSWVDGVQIHRFAPTPKPFRRDEVSFVGLNSYAVGSQ
CEPEPDADVLRSMILTDPHITAETAARRLARGSPPEASSSVSLSAPSLRATCTTHSNTYDV
DMVDANLLMEGGVAQTEPESRVPVLDLFLEPMAEEESDLEPSIPSECMLPRSGFPRALPAWAR
PDYNPPLVESWRRPDYQPPTVAGCALPPPCKAPTPPRRRRRTVGLSESTISEALQQLAIKTFG
QPPSSGDAGSSTGAGAAESGGPTSPGEPAPSETGSASSMPPELEGEPGDPDLESDQVELQPP
PQGGGVAPGSGSGSWSTCSEEDDTTVCC

NS5B HCV Genotype 2A

SMSYSWTGALITPCSPEEEKLPINPLSNLLRYHNKVYCTTSKSASQRAKKVTFDRTQVLDAH
DSVLKDIKLAASKVSARLLTLEEACQLTPPHSARSKYGFGAKEVRSLSGRAVNHKSVWKDLE
DPQTPIPTTIMAKNEVFCVDPKAGGKPPARLIVYPDLGVRVCEKMALYDITQKLPQAVMGASYG
FQYSPAQRVEYLLKAWAEKKDPMGFSYDTRCFDSTVTERDIRTEESIQACSLPEEARTAIHSL
TERLYVGGPMFNSKGQTCGYRRCRASGVLTTSMGNTITCYVKALAACKAAGIVAPTMLVCGD
DLVVISQSGTEEDERNLRAFTEAMTRYSAPPGDPPRPEYDLELITSCSSNVSVALGPRGRRR
YYLTRDPTTPLARA AWETVRHSPINSWLGNIQYAPTIWVRMVLMTTHFFSILMVQDTLDQNLNF
EMYGSVYSVNPLDLPALIERLHGLDAFSMHTYSHHELTRVASALRKL GAPPLRVWKSRRARAVR
ASLISRGGKAAVCGRYLFNWAVKTKLKLTPPEARLLDLSSWFTVGAGGGDIFHSVSRARPRSL
LFGLLLLFVGVGLFLLPAR

Hs_VAPA

MAKHEQILVLDPPTDLKFKGPFTDVVTTNLKLRNPSDRKVCFKVKTAPRRYCVRPNNGIIDPG
STVTVSVMLQPFYDPNEKSKHKFMVQTFAPNTSDMEAVWKEAKPDELMDSKLRCVFEMP
NENDKLNDEPSKAVPLNASKQDGPMPKPHSVSLNDTETRKLMEECKRLQGEMMKLSEENR
HLRDEGLRLRKAHSDKPGSTSTASFRDNVTSPLPSLLVIAAIFIGFFLGKFIL

Hs_VAPB

MAKVEQVLSLEPQHELKFRGPFTDVVTTNLKLGNPTRDNRVCFKVKTTAPRRYCVRPNNGIIDAG
ASINVSVMMLQPFYDPNEKSKHKFMVQSMFAPTDTSMEAVWKEAKPEDLMDSKLRCVFELP
AENDKPHDVEINKIISTTASKTETPIVSKSLSSSLDDTEVKKVMEECKRLQGEVQRLREENKQFK
EEDGLRMRKTVQSNPISALAPTGKEEGLSTRLLALVVLFFIVGVIIKIAL

Hs_WIBG

MEAAGSPAATETGKYIASTQRPDGTWRKQRRVKEGYVPQEEVPVYENKYVKFFKSKPELPPG
LSPEATAPVTPSRPEGGEPGLSKTAKRNLKRKEKRRQQQEKGEAEALSRTLDKVSLEETAQLP
SAPQGSRAAPTAASDQPSAATTEKAKKIKNLKKLQRQVEELQQRIQAGEVSQPSKEQLEKLA
RRRALEEELEDLELGL

Affinity Purification for Mass Spectrometry

Cells were lysed in IP buffer with detergent (150mM NaCl, 50mM Tris pH 7.4, 1mM EDTA, 0.5% NP-40 substitute) for 30 min at 4°C and passed 10 times through a G23 needle. Clarified lysates were affinity-purified with Streptactin Superflow Resin for strep-tagged proteins (IBA, 2-1206-025) or Anti-flag M2 affinity gel for flag-tagged proteins (Sigma, A2220) at 4°C overnight. For immunoprecipitations of native proteins in replicon-expressing cells, antibodies recognizing VAPA or HCV NS5A were incubated with lysates at 4°C overnight. To precipitate antibody-protein complexes, we added 50ul of a Protein A/G agarose slurry. Resin was washed four times in IP

buffer with detergent, followed by two washes in IP buffer without detergent (150mM NaCl, 50mM Tris pH 7.4, 1mM EDTA). Resin was resuspended in 40µl IP buffer without detergent containing 2mM biotin for strep-tagged proteins or 0.1 mg/ml 3X flag peptide (Sigma, F4799) and 0.05% Rapigest (Waters) for flag-tagged proteins at 4°C for 30 minutes, with agitation. We reserved 20 µl of the for analysis by SDS-PAGE followed by either western blotting using infrared detection (Li-Cor Biosciences) or silver staining (Thermo Scientific, 24600).

Sample Preparation for Mass Spectrometry

Purified proteins eluates were digested with trypsin for LC-MS/MS analysis. Samples were denatured and reduced in 2M urea, 10 mM NH₄HCO₃, 2 mM DTT for 30 min at 60C, then alkylated with 2 mM iodoacetamide for 45 min at room temperature. Trypsin (Promega) was added at a 1:100 enzyme:substrate ratio and digested overnight at 37C. Following digestion, samples were concentrated using C18 ZipTips (Millipore) according to the manufacturer's specifications. Desalted samples were evaporated to dryness and resuspended in 0.1% formic acid for mass spectrometry analysis.

Mass Spectrometry

Digested peptide mixtures were analyzed by LC-MS/MS on either a Thermo Scientific LTQ XL linear ion trap mass spectrometer or a Thermo Scientific Velos Pro dual linear ion trap mass spectrometer. The LTQ XL system was equipped with a LC Packings UltiMate HPLC with an analytical column (10 cm x 75 µm I.D. packed with ReproSil Pur C18 AQ 5 µm particles) and the Velos Pro system was equipped with a Proxeon Easy-nLC HPLC with a pre-column (2 cm x 100 µm I.D. packed with ReproSil Pur C18 AQ 5 µm particles) and an analytical column (10 cm x 75 µm I.D. packed with ReproSil Pur C18 AQ 3 µm particles). Both systems delivered a gradient from 5% to 30% ACN in 0.1% formic acid over one hour. Both mass spectrometers collected data in a data-dependent fashion. The LTQ XL collected one full scan followed by 10 collision-induced

dissociation MS/MS scans of the 10 most intense peaks from the full scan. The Velos Pro collected one full scan followed by 20 collision-induced dissociation MS/MS scans of the 20 most intense peaks from the full scan. Dynamic exclusion was enabled on both systems for 30 seconds with a repeat count of 1. Data were searched against a database containing SwissProt Human protein sequences (downloaded March 6, 2012) and HCV sequences, concatenated to a decoy database where each sequence was randomized in order to estimate the false positive rate. The searches considered a precursor mass tolerance of 1 Da and fragment ion tolerances of 0.8 da, and considered variable modifications for protein N-terminal acetylation, protein N-terminal acetylation and oxidation, glutamine to pyroglutamate conversion for peptide N-terminal glutamine residues, protein N-terminal methionine loss, protein N-terminal acetylation and methionine loss, and methionine oxidation, and constant modification for carbamidomethyl cysteine. The resulting raw data was matched to protein sequences by the Protein Prospector algorithm. Data were searched against a database containing SwissProt Human protein sequences (downloaded March 6, 2012) and HCV sequences. Prospector data was filtered using a maximum protein expectation value of 0.01 and a maximum peptide expectation value of 0.05.

Native VAPA and HCV NS5A Mass Spectrometry and Analysis

Purified proteins were digested as described above. Digested peptide mixtures were analyzed by LC-MS/MS on a Thermo Scientific LTQ Orbitrap Elite mass spectrometry system equipped with a Proxeon Easy nLC 1000 ultra high-pressure liquid chromatography and autosampler system. Samples were injected onto a C18 column (25 cm x 75 μ m I.D. packed with ReproSil Pur C18 AQ 1.9 μ m particles) in 0.1% formic acid and then separated with a one-hour gradient from 5% to 30% ACN in 0.1% formic acid at a flow rate of 300 nl/min. The mass spectrometer collected data in a data-dependent fashion, collecting one full scan in the Orbitrap at 120,000 resolution followed by 20 collision-induced dissociation MS/MS scans in the dual linear ion trap for the 20 most intense peaks from the full scan. Dynamic exclusion was enabled for 30 seconds with a repeat count of

1. Charge state screening was employed to reject analysis of singly charged species or species for which a charge could not be assigned. The raw data was matched to protein sequences by the MaxQuant algorithm (version 1.3.0). Data were searched against a database containing SwissProt Human and hepatitis C virus protein sequences, concatenated to a decoy database where each sequence was randomized in order to estimate the false positive rate. Variable modifications were allowed for methionine oxidation and protein N-terminus acetylation. A fixed modification was indicated for cysteine carbamidomethylation. Full trypsin specificity was required. The first search was performed with a mass accuracy of ± 20 parts per million and the main search was performed with a mass accuracy of ± 6 parts per million. A maximum of 5 modifications were allowed per peptide. A maximum of 2 missed cleavages were allowed. The maximum charge allowed was 7+. Individual peptide mass tolerances were allowed. For MS/MS matching, a mass tolerance of 0.5 Da was allowed and the top 6 peaks per 100 Da were analyzed. MS/MS matching was allowed for higher charge states, water and ammonia loss events. The data were filtered to obtain a peptide, protein, and site-level false discovery rate of 0.01. The minimum peptide length was 7 amino acids. Results were matched between runs with a time window of 2 minutes for technical duplicates.

The data was analyzed using the MSstats package (Choi et al., 2014) in R/Bioconductor (v.2.3.4). To prepare the data for analysis, the set of identified peptides by MaxQuant (Cox and Mann, 2008) was filtered for contaminants and false positives from the search. The affinity purification and control sample intensities were then log₂-transformed and normalized using GAPDH and MYH9 as global standards across runs. Missing intensity values for peptides were imputed by using the mean minimum intensity across all MS runs. The significance of the fold-change for every protein between pull-down and control was tested using mixed effect models, implemented in the group comparison function of MSstats, with no equal feature variance and restricted scope of technical and biological replication. Statistically significant interaction partners were selected

by filtering results on a log₂-fold-change > 2 and adjusted p-value (or False Discovery Rate) < 0.05.

Interactome scoring and visualization

The first iteration of the HCV interactome was compiled through selecting bait-prey pairs with a MIST score > .70, computed with the previously published feature weights for reproducibility (.31), abundance (.01) and specificity (.68) (Jager et al., 2011), or a top 5% Comppass WD score per bait (Sowa et al., 2009). The new weights for the MIST score, MIST threshold and Comppass threshold were derived by testing the prediction performance of the top 10 optimal weight combinations, trained on two thirds of a benchmark set containing 5200 interactions (52 positive interactions and 5148 negative interactions randomly sampled from the mass-spectrometry results). The prediction performance was tested on a validation set composed of the remaining one third of 5200 benchmark interactions. To explore many putative score configurations, an exhaustive grid search was performed on the 4-dimensional vector described by the 3 weight variables and a threshold variable. The domain of these variables was limited to the discrete range between 0 and 1, with 0.01 increments. The sum of the three weight variables was constrained to 1. For every complete assignment of the variable vector, the True Positive Rate (TPR) and False Positive Rate (FPR) were computed to plot a Receiver Operating Curve (ROC) on the validation set. Both the ROC curve and the F1-score, the harmonic mean of precision and sensitivity, were used to select the optimal combination of MIST weights, MIST threshold and Comppass threshold. The refined interactome was compiled through selecting bait-prey pairs with a retrained MIST score > 0.68, using new weights for reproducibility (.36), abundance (.09) and specificity (.55), or a top 1% Comppass WD score per bait. The final iteration of the HCV-interactome was visualized as network representations using Cytoscape, version 2.8.3 (Smoot et al., 2011).

Functional and domain ontology enrichments

For each bait, the average MIST score of terms (GO-BP, GO-MF, KEGG, PFAM and Uniprot), that have at least one associated protein interacting with the bait, was compared to a distribution of averages taken from randomly sampled protein-term associations of the same size. The p-value that the actual term score is higher than the distribution of sampled scores was computed by the one-tailed cumulative normal distribution test. All the p-values were adjusted for multiple hypotheses testing by applying the Benjamini-Hochbach correction to obtain q-values. Terms with q-values < 0.05 were reported as output and visualized as heat maps using the R package. GO-BP, GO-MF and KEGG terms were joined into a functional ontology. PFAM and Uniprot terms were joined into a domain ontology. (Table S7).

Lentivirus Production and Transductions

Lentiviral particles were produced as described (Lai and Brady, 2002). Briefly, 293T cells were co-transfected with the transfer plasmid encoding shRNA constructs, an HIV-based packaging construct (pCMVΔR8.91), and a construct expressing the glycoprotein of vesicular stomatitis virus (VSV-G) (pMD.G). Culture supernatants containing pseudotyped lentiviral particles were stored at -80°C. Cells were transduced in the presence of 8 µg/ml Polybrene (Sigma) for 24 hours at 37°C.

In Vitro Transcription of HCV RNA, Electroporations, and HCV storage

Plasmids encoding HCV reporters were *in vitro* transcribed using the MegaScript T7 kit (Ambion) according to the manufacturer's protocol. For RNA electroporation, Huh7.5 cells were trypsinized, washed once in Opti-MEM (Invitrogen) and resuspended in Cytomix buffer (120 mM KCl, 5 mM MgCl₂, 0.15 mM CaCl₂, 2 mM EGTA, 1.9 mM ATP, 4.7 mM GSH, 25 mM HEPES, 10 mM potassium phosphate buffer, pH 7.6) at 10⁷ cells ml⁻¹. 400 µl of the cell suspension was mixed with 10 µg of HCV RNA and pulsed at 260 V and 950 microfarads with the Gene Pulser II (Bio-Rad) and incubated for 6 days at 37°C. Using this method, we obtained a supernatant with

~10,000 focus-forming units (ffu)/ml. Freezing of HCV particles is challenging and usually associated with a dramatic loss in infectivity of the viral stock. However, following a protocol by Yi, M. (Yi, 2010) we froze our viral stocks at -80°C with 20% fetal bovine serum (FBS), which preserves infectivity after one freeze-thawing cycle to almost 100%.

HCV Infections and Replicon Experiments

Following lentiviral infection, host protein-depleted Huh7.5 cells were split into 48-well plates at two different cell densities of 10,000 and 20,000 cells/well in triplicates. Scramble shRNA-transduced cells were seeded at varying cell densities of 1000 to 40,000 cells/well to generate a standard curve of infection (see main text). Cells were infected with a monocistronic infectious clone of HCV_{Jc1} encoding orange fluorescent protein (OFP) and a blastocidin-resistance gene (BSD) at an MOI of 0.03 or 0.06. The OFP-Bsd fusion protein is excised after infection and functions as a fluorescent marker for infected cells and a resistance gene to select for infected cells. Following infection with HCV, cells received fresh media 1 day and 4 days post HCV infection. After 6 days of infection, the cells were washed with PBS, detached by adding 200 µl of trypsin, and fixed with 200 µl of 4% paraformaldehyde and analyzed by flow cytometry. The standard curve was used to determine an expected infection rate given the cell density for each sample and the ratio of actual vs. expected rate of infection was generated. A 25% decrease (<0.75) or increase (>1.25) in the ratio as compared to the scramble controls indicated a phenotype for a given sample. HCV infections to analyze levels of nonsense-mediated decay substrates were conducted with two additional virus constructs: an untagged Jc1 virus and a super-infectious monocistronic Jc1 virus (Jc1/^{NS5AB-OFP-Bsd}) that has been previously described (Webster et al., 2013). For HCV replicon experiments, Huh7.5 cells were electroporated with monocistronic Jc1 HCV as described above but with a deletion of the E1 and E2 genes Jc1^{ΔE1E2/NS5AB-OFP-Bsd}. Cells were selected with blasticidin for one week to obtain a replicon-expressing cell line.

Quantitative RT-PCR

The SYBR green qPCR reactions contained 5 µl of 2x Maxima SYBR green/Rox qPCR Master Mix (Thermo), 5 µl of diluted cDNA, and 5 pmol of both forward and reverse primers. The reactions were run using the following conditions: 50°C for 2 min, 95°C for 10 mins, followed by 40 cycles of 95°C for 5 secs and 60°C for 30 secs.

Primers for qPCR		
Gene	Forward primer	Reverse primer
18S rRNA	AACCCGTTGAACCCCAT	CCATCCAATCGGTAGTAGCG
HCV CORE	ATCCCTAAAGATCGGCGCTCCAC	AGCCGCACGTTAGGGTATCGATG
AASDHPPT	TGGCTGGTCTGCTGATGATAA	TCGGGTAAGGATTCGATGAGT
ACTG1	CCGAGCCGTGTTTCTTCC	GCCATGCTCAATGGGGTACT
ADE2	TTGCAGAAGAATAGCAACTGGTT	CACTGTGGGTCATTATTGGCAT
AIMP1	GGTACTCCACTGCACGCTAAT	CCAGAAGATACGGTTGTTACTGC
AMBP	CTCTCGGATCTATGGGAAGTGG	CGTGCTCACTGTCATCCTGTC
ANKRD28	AATTGCTTGTGTGCGATGGAG	TAGCAGGCTACATGAAGAGGT
ARIDRA	ACCACGGCGACTGGACTTA	CACAGGTGTCCCTCGCTTC
ARL8B	CATCGCGTCAGGTCAATTCAAG	GTTGTCTCTCTATGTCCCAGA
ASNS	GGAAGACAGCCCCGATTTACT	AGCACGAACTGTTGTAATGTCA
AT2C1	TGATGATGCCGTCAGTATCACT	CCTTCACGCACACAATGGC
BAG6	AGTGTCCACGCATCCGTAG	CCCAAACAGTGAGTTTCTGAGG
BIN1	TGAGCAGTGCGTCCAGAATTT	CGATCTTGTGGCTCATCCC
CAD	AGTGGTGTTCAAACCGGCAT	CAGAGGATAGGTGAGCACTAAGA
CARS	CCATGCAGACTCCACCTTTAC	GCAATACCACGTCACCTTTTTTC
CHCHD2	ACACATTGGGTCACGCCATTA	GCACCTCATTGAAACCCTCACA
CHCHD3	GAGGCGGACGAGAATGAGAAC	ACCAGAATACCGCTGAGACTTC
CLEC16A	ATGGCAAGACTTCCCGCAA	CACGTAACGGCCCGACTTTT
COG1	GCCGAGATCGAGCACAAGAA	GGCAGCCATGCTGTAGAACT
COG3	AGAAAGAATTGAAACCGCACAGC	GCTTCATGTAGGGTTCTGTCT
COG8	CGACTTGGCCTTCGCTAACTA	TAGGGTCAGGCTATTCATCCG
CSNK2A1	GGTGAATGGGAAATCAAGAT	TGATGATGTTGGGACCTCCTC
CW19L2	AGTGGTAGATTTGAAAGTGCGAA	AGCATCCATGTATCCTCACCC
CYB5B	ATGTCCGGTTCAATGGCGAC	CATGGATCACAAGCCACAGTT
DDX1	TCTCCGAGATGGGTGTAATGC	ACCTCCTCCTAAGATCAATGGG
DDX21	GAGGAGCCATCTCAAATGACA	GGGTTACAGTCCGGTTCAGG
DDX3X	AGCAGTTTTGGATCTCGTAGTG	ACTGTTTCCACCACGTTCAAAT
DDX52	ACGTCCACGATCTCTTTCGC	TGAAGCACCTCCGAAGAATCA
DECR1	TCTTCAAAAAGCGATGCTACCA	CTATCACGCACTGAGCACCT
DERL2	TTTTTGGGCCAGTTGGATTCA	GCTCCACACATAGACGAGCATTA

DGAT1	TATTGCGGCCAATGTCTTTGC	CACTGGAGTGATAGACTCAACCA
DNAJB11	AACCTGAGCACCTTTTGCT	GGTTCCGGTCGGGATGAAG
DNAJB4	GCAGGAGGTACTGATGGACAA	ACCACCCATTGCTCTTCCAAA
DNAJC7	AGCTATTATGGTAATCGAGCAGC	CTTCCCGGAACCTTCCAAGC
DOCK9	TGTCATCGTCCAGAAGAAGACT	TCTCAGGATGGCCGTCTGAAA
EMID2	CTGCGCCAACCTCGTAAGG	TTCCTCATCACAGTTGCTCCC
F213A	ATGGGGATGTGGTCCATTGG	GCACGGCCATAATCACAGC
FNDC3B	TCTCGTTCAAGTTAATCCAGGTG	ACATGGCTGAGGGGTAGCTT
FXR2	GGGCCTTCTACAAGGGCTTTG	TCTCTCACTCTGCCAGTTGTT
GAPDH	TGCCAAATATGATGACATCAAGAA	GGAGTGGGTGTCGCTGTTG
GCSH	GGAAGCGTTGGGAGATGTTGT	TCTGAAGGGTTACTCAGTGTC
GGCX (VKGC)	ATGGTGCTAGACATTCCCCAG	GATACATCCAGTCAAGTGGCAG
GNG12	AGCAAGCACCAACAATATAGCC	AGTAGGACATGAGGTCCGCT
GNG5	CAACCGCGTAAAAGTTTCCCA	GGGTCATGTTGAGCATTCTGC
GOLGA2	CCC CGCATGTCGGAAGAAA	GCATTGTCCTTGGGTGTATCCT
GPR89C	TGACTCTCATGGCTCTTCTTTC	ATATCCGTGTCAGTCACATTCC
HCCS	ATGAAAGGCTGTCCAGTGAATAC	GGTGGCATCAGATTTGAAGGAT
HNRNP2	AGTGATGCGCTTCTTCTCTGA	TTCGGACCTGTATGCTTCAAC
HPRT1	CCTGGCGTCGTGATTAGTGAT	AGACGTTCAAGTCTGTCCATAA
HSD17B10	TGGCGGTAATAACCGGAGGA	ACAGTTGACAGCTACATCCACA
IFT88	GGGTCCAAGACATCTCTGGC	CATGGGTCTAGTAACTCCATCCT
IMP3	CCCTGACGTGGTTACCGAC	CCGCTTGATCTTGGACGAGT
KHSRP	ATCCGCAAGGACGCTTTTCG	GGAGTGCTGTTATTCACTGTCCG
LDHA	ATGGCAACTCTAAAGGATCAGC	CCAACCCCAACAACGTAAATCT
LMF2	CTCACCTACCACTACGAGACC	GCACAGCGATCTCAATTAGGAAG
LPCAT1	CGCCTCACTCGTCTACTTC	TTCCCCAGATCGGGATGTCTC
LRC18	GCGCCTTAGTGACATGGAC	GGCAGCTTGCTATGTAGTTGC
LRRC59	TGACTACTCTACCGTCGGATTT	TTCAGGTCCAACCACTTCAGG
LUC7L	ACGGAGATACAACCTCGTCAACG	AGGTGACTCTTGCACTACTCTGT
Marcks-related protein	CAAGGGTGAAGGGGAGTCCG	GACAGGCCGCTCAATTTGAAA
MCM2	ATGGCGGAATCATCGGAATCC	GGTGAGGGCATCAGTACGC
MAGOH	TTTATCTGCGTTACTACGTGGGG	CGTCCGGTCGAAACTCAAAC
MIF	ATCAGCCCGGACAGGGTCTACATCAA	TTAGGCGAAGGTGGAGTTGTTCCA
MOGS	CCGGGGACTCCTAAGCTCA	CCTCTTGACGAACTCAGTGGT
MRS2	ACTTAGAGCAATGGCTGTTCC	GCATCCAAGGTCTCAAGGATCAG
MSI2H	ACCTCACCAGATAGCCTTAGAG	AGCGTTTCGTAGTGGGATCTC
MTX2	GCCTTCGTCTCCAGATTGC	AGAGAAGCTGCATTGTCAGAAAG
NAP1L1	AAAGCACGTCAGCTAACTGTT	TTGAGAGCATTCACTCGTCTTTT
NAP1L4	TCCAGCTACATCGAACTTTACC	ACATCGCCGGTGATAAATTCTC
OAT	GTGGGGCTATACCGTGAAGG	TGGTCCAAAACCATCGTAACTG
PEF1	AGGGCAGTATGGTAGTGGG	GGCACCGTAGGAACTTGGA
PEG10	AGCAGTCGGAGGAGAACAAC	CACTGGGCCATGAAAGGAG

PIGS	GCGGCTACACACCTAGAGG	CTGGGAGTAAGGCAACGAGG
PP2AB	CTGAACGAGAACCAAGTGCG	ACGAACCTCTTGACATTTGA
PPIA	CCCACCGTGTTCCTTCGACATT	GGACCCGTATGCTTTAGGATGA
PRDX1	CCACGGAGATCATTGCTTTCA	AGGTGTATTGACCCATGCTAGAT
PHB2	GTGCGCGAATCTGTGTTTAC	GATAATGGGGTACTGGAACCAAG
PSMA5	TGCCATGAGTGGGCTAATTG	GGCACCTGGATCTGCATCTT
PSMC3	CGAGCAAGATGGAATTGGGGA	GCTCATGGGTGACTCTCAACA
PSME2	GCAAGAGGACTCCCTCAATGT	CTTCTGGCTTAACCAGGGCA
Rab5C	CCGCTTTGTCAAGGGACAGTT	AGGCTGTGATACCGCTCCT
RAP2C	TCTACCGCAAAGAGATCGAAGT	ACCTTGGCCGTTTTTGTATGA
RM22	CGAGGAATGTCTATTGACCAGGC	CGGATGCGTTTCAGGCACT
RNF5	GCCAGAACGGCAAGAGTGT	GGCTCCCTCGCCATAAAG
RPA1	GGGGATACAAACATAAAGCCCA	CGATAACGCGGCGGACTATT
RPA3	AGCTCAATTCATCGACAAGCC	TCTTCATCAAGGGGTTCCATCA
RPLP1	AGCCTCATCTGCAATGTAGGG	TCAGACTCCTCGGATTCTTCTTT
RRP1	CAGGTGGTTTTACGCACGAC	GAACGAGCTGGGAAATAGTCC
RT18C	GTTTGCGGTGGTCTAGGGAG	TGCTGGATACCTGTTGTGAAC
RTN3	ACTGGGTTTGTCTTTGGCAC	ATGACGGACTTGTAGATCCTGA
RUVBL1	AGGTGAAGAGCACTACGAAGA	CTACTATGACGCCACATGCCT
RUVBL2	AAGTCCCGGAGATCCGTGAT	CACCGATTGCTCAATCCTTG
SACM1L	GCTGAAGCTGCATATCACACC	ACGGTCAATGGTAAGTACGTCA
SC35-1.6kb	CGGTGTCCTC TTAAGAAAATGATGTA	CTGCTACACA ACTGCGCCTT TT
SCAMP3	AGGAGTTGGACCGAAGGGAG	GGCAGCGGAGGAAGTTTCAAG
SCMC1	GGTGTCTGTCTCTCGAACAAG	CATCTGTGCGAAAGCCACCAAA
SEC63	TCGTGATCCCGGCGACATA	AAACGATACCACATACACCTTCC
SHRPN	GGGGCGGTTAATTTGGAGTG	CTCGGACTAGGACTGCCCA
SLC16A1	AGGTCCAGTTGGATACACCCC	GCATAAGAGAAGCCGATGGAAAT
SLC25A12	TCAAGGTGCAGACAACCTAAGC	GGGGTCATATAACGCTCTCCA
SLC25A24	GGTGTCTGTCTCTCGAACAAG	CATCTGTGCGAAAGCCACCAAA
SSBP1	TGAGTCCGAAACAACCTACCAGT	CCTGATCGCCACATCTCATTAG
STX18	ATCACGCTGCTATTCCGGG	TCCTCCCATATTCAGACATGGT
TBRG4	CAGCTCACCTGGTAAAGCGAT	GGGAGTAGATGCTCGTTCCTTC
TCP ALPHA	CCAGCCACGCTATCCAGTC	TCAAGGCAAGCAATTTTTGCAT
TCP BETA	ATTGGAGACTTGGTAAAGAGCAC	TCTCGTCCACTGCTTAGAAGA
TCP DELTA	ATGCCCGAGAATGTGGCAC	GCTTGTGCGGGTCTGATAG
THOC3	TCGGGGTCTTCGACAAGA	CTGGTCCACACTATCCCAT
Timm13	CAGAGGATGACGGACAAGTGT	CATGTAGCGGTCCATGCACA
TM9S4	GATTGGTTGCCGTGGTCTTTA	TTCTACGGGATCGTTCTGGTG
TMPO	CCCCTCGGTCTGACAAAAG	CGCTCTTCGCTACTGGAGAA
TMX3	GGGCCTTCTACAAGGGCTTTG	TCTCTACTCTGCCAGTTGTT
TNPO1	CTGTGAGGGAGCATTTGGTG	TGTGCAACATTAGAGCTTGAGTC
TRX5	CAACAGAGGGAACAGGAACGA	CCAGGTCATTCCAAGTCGGC
UBE2G2	ATCTACCCTGATGGGAGAGTCT	CTCCACTTTCGTCATTGGGC

UBE2O	ACTAGAGGACCGTTCTGTGGT	TGACGGGATAGATGATGCAGTT
UBE2S	ACAAGGAGGTGACGACACTGA	CCACGTTCCGGTGGAAGAT
UBL4A	AGATGGGAAACGACTCTCGGA	CCACTAGGTTGAGCTTGGAGTT
UBR5	GTCCATCCATTTCTGTGGTTCA	CCAATCCAATCTGTCTGGCTG
UPF1	ACCGACTTTACTCTTCTAGCC	AGGTCCTTCGTGTAATAGGTGTC
UPF2	GGAGAAAACACCTAACATCACCA	CCTTGTCAGTGAAAATCCCAACT
USP19	AAAGTGCAAACCCGCAAGG	AGTTCAGCGGTGGTATGCAAA
VAPA	AGATCCTGGTCTCGATCCG	TTTTCTATCCGATGGATTTTCGCA
VAPB	AGATGGACTGCGGATGAGGAA	CAGTTGGGGCTAATGCTGAAA
VCP	GCCGATTCAAAAGGTGATGACC	CGATTGGGACGGTTCTTCTGT
VDAC1	ACGTATGCCGATCTTGGCAAA	TCAGGCCGTA CT CAGTCCATC
VDAC2	GGCGTGGAATTTTCAACGTCC	AGACCATACTCACACCACTTGTA
WDR18	TCGTGTGGGAACTTCACTCG	CATTGGGTGATGCAGTCAGAC
WIBG	GGCAAGTATATCGCGTCAACA	TTCAGGTTACGTTTGGCTGTC
XKR7	GCGCTGCTCGTGTTCTTCT	CGAGTAGTCGTAGACGAACCA
YWHAQ	AGGGTCATCTCTAGCATCGAG	CCACTTTCTCCCGATAGTCCTT
ZW10	ATGGCCTCGTTCGTGACAG	CAGATAGCTTATCCACCTGGGTA

Immunoprecipitations and Western Blots

Cells were lysed in RIPA buffer (50mM Tris-HCl, pH 8, 150mM NaCl, 1% NP-40, 0.5% sodium deoxycholate, 0.1% SDS, supplemented with protease inhibitor cocktail (Sigma)) or IP Buffer (150mM NaCl, 50mM Tris pH 7.4, 1mM EDTA, 0.5% NP-40 substitute, supplemented with protease inhibitor cocktail (Sigma)) for 30 min at 4°C and passed 10 times through a G23 needle. Clarified lysates were immunoprecipitated with Flag M2 agarose (Sigma) or HA agarose (Sigma) overnight, washed four times in lysis buffer, and resuspended in Laemmli buffer for SDS-PAGE. For immunoprecipitations of endogenous WIBG in HCV-infected, antibodies recognizing WIBG were incubated with lysates at 4°C overnight. To precipitate antibody-protein complexes, we added 50ul of a Protein A/G agarose slurry and eluted as above. For chemiluminescent detection, we used ECL and ECL Hyperfilm (Amersham).

Antibodies The following primary antibodies were used: α -flag (F7425, Sigma), α -COXIV (ab16056, Abcam), α -calreticulin (SPA-600, Stressgen), α -V5 (A190-120A, Bethyl), α -Strep-tag II (ab76949, Abcam), α -CYB5B (HPA007893, Sigma), α -tubulin (ab15246, Abcam), α -HA

(11867423001, Roche), α -WIBG (SAB1103121, Sigma), α -WIBG (70R-10101, Fitzgerald) α -Magoh (sc-271365, Santa Cruz Biotechnology Inc.), and α -RBM8A (Y14) (HPA018403, Sigma), α -VAPA (A304-366A, Bethyl Laboratories, Inc.), α -NS5A (HCM-131-5, Austral Biologicals).

Mitochondrial Enrichment

Mitochondria were isolated from HEK293T cells using the Mitochondrial Isolation Kit for Cultured Cells and lysis of cells was done with 10 μ l Reagent B. Cellular debris was removed by two sequential centrifugations at 700 x *g* for 10 minutes at 4°C, discarding the pellet after each spin. Mitochondria were pelleted by centrifugation at 3,000 x *g* for 15 minutes at 4°C. The pelleted mitochondria were washed, resuspended in 100 μ l of Reagent C. Supernatants were cleared of mitochondrial contamination by two sequential centrifugations at 12,000 x *g* for 15 minutes at 4°C, reserving the supernatant as the cytoplasmic fraction.

Mitochondrial Viability Assays

For mitochondrial factors influencing HCV infection, we selected the two shRNAs yielding the most significant alteration of HCV infection. Following lentiviral infection, host protein-depleted Huh7.5 cells were plated in triplicate in 96-well plates at a density of 40,000 cells per well. For the alamar blue assay, cells were incubated with 200 μ l alamar blue reagent and percent reagent reduction was calculated according the manufacturers intructions (Thermo Scientific alamarBlue Cell Viability Assay Reagent, Cat.# 88951). For the CMXRos assay, cells were incubated in DMEM containing 200nM CMXRos for 30 minutes at 37°C. Cells were washed with PBS, trypsinized and transferred to a 96-well V-bottom plate, then pelleted and resuspended in PBS. Mean fluorescence intensity was measured by flow cytometry. For both assays scramble shRNA was used as a negative control and CCCP at a final concentration of 50 μ M was used as a positive control.

Supplemental References

Choi, M., Chang, C.Y., Clough, T., Broudy, D., Killeen, T., MacLean, B., and Vitek, O. (2014).

MSstats: an R package for statistical analysis of quantitative mass spectrometry-based proteomic experiments. *Bioinformatics* 30, 2524-2526.

Cox, J., and Mann, M. (2008). MaxQuant enables high peptide identification rates, individualized p.p.b.-range mass accuracies and proteome-wide protein quantification. *Nat Biotechnol* 26, 1367-1372.

Jager, S., Cimermancic, P., Gulbahce, N., Johnson, J.R., McGovern, K.E., Clarke, S.C., Shales, M., Mercenne, G., Pache, L., Li, K., *et al.* (2011). Global landscape of HIV-human protein complexes. *Nature* 481, 365-370.

Lai, Z., and Brady, R.O. (2002). Gene transfer into the central nervous system in vivo using a recombinant lentivirus vector. *J Neurosci Res* 67, 363-371.

Li, M.Z., and Elledge, S.J. (2012). SLIC: a method for sequence- and ligation-independent cloning. *Methods Mol Biol* 852, 51-59.

Smoot, M.E., Ono, K., Ruscheinski, J., Wang, P.L., and Ideker, T. (2011). Cytoscape 2.8: new features for data integration and network visualization. *Bioinformatics* 27, 431-432.

Sowa, M.E., Bennett, E.J., Gygi, S.P., and Harper, J.W. (2009). Defining the human deubiquitinating enzyme interaction landscape. *Cell* 138, 389-403.

Webster, B., Ott, M., and Greene, W.C. (2013). Evasion of superinfection exclusion and elimination of primary viral RNA by an adapted strain of hepatitis C virus. *J Virol* 87, 13354-13369.

Yang, X., Boehm, J.S., Yang, X., Salehi-Ashtiani, K., Hao, T., Shen, Y., Lubonja, R., Thomas, S.R., Alkan, O., Bhimdi, T., *et al.* (2011). A public genome-scale lentiviral expression library of human ORFs. *Nat Methods* 8, 659-661.

Yi, M. (2010). Hepatitis C virus: propagation, quantification, and storage. *Curr Protoc Microbiol* Chapter 15, Unit 15D 11.

